Articles

Predicting Guest Orientations in Layered Double Hydroxide Intercalates

Andrew M. Fogg,[†] Andrew L. Rohl,*[,‡] Gordon M. Parkinson,*[,‡] and Dermot O'Hare*[,†]

Inorganic Chemistry Laboratory, University of Oxford, South Parks Road, Oxford, OX1 3QR, UK, and A. J. Parker Cooperative Research Centre for Hydrometallurgy, School of Applied Chemistry, Curtin University of Technology, P.O. Box U 1987, Perth 6845, Australia

Received February 1, 1999

Molecular mechanics have been used to rationalize the structures of the layered double hydroxide intercalates $[LiAl_2(OH)_6]Cl$, $[LiAl_2(OH)_6]Br$, and $[LiAl_2(OH)_6]NO_3$. The simulations showed that calculated lowest energy structures were in good agreement with the experimentally determined structures and were able to explain the positional disorder of the NO_3^- guest anions found in the structure of $[LiAl_2(OH)_6]NO_3$. Furthermore, the calculations also proved to be a useful predictive tool for the interlayer spacing and consequently the guest orientation in the related intercalates $[LiAl_2(OH)_6]_2CO_3$, $[LiAl_2(OH)_6]_2SO_4$, and $[LiAl_2(OH)_6]_2C_2O_4$, for which the structures have not been determined by conventional diffraction techniques.

Introduction

Layered double hydroxides are a class of intercalation compounds with positively charged layers consisting of two metal cations octahedrally coordinated by hydroxide groups. Charge neutrality is maintained by interlayer anions, which are frequently labile, giving rise to numerous anion exchange derivatives. They have found widespread applications as anion scavengers, flame retardants and flame proof coatings,[1] drug supports,[2] and in catalysis.[3]

Aluminum hydroxide, $Al(OH)_3$, exists in nature as three structural modifications: gibbsite, bayerite, and nordstrandite.[4−7] In gibbsite, each of the $Al(OH)_3$ layers consists of nearly close-packed OH^- ions in which the Al^{3+} ions occupy two-thirds of the octahedral holes between alternate layers. Reaction of gibbsite with LiCl yields the layered double hydroxide $[LiAl_2(OH)_6]Cl{\cdot}H_2O$. A combined synchrotron X-ray and neutron diffraction Rietveld refinement of this intercalate and the dehydrated analogues $[LiAl_2(OH)_6]X$ ($X = Cl^-$, Br^-, NO_3^-) has recently been performed.[8] In all cases, the $[LiAl_2(OH)_6]^+$ layers are eclipsed along the *c*-axis with the Li^+ cations occupying the vacant octahedral holes in the $Al(OH)_3$ layers, and the anions are located in the interlayer region. In the dehydrated compound, $[LiAl_2(OH)_6]Cl$, the Cl^- anions are ordered so that they form ···Li···Cl···Li···Cl··· chains through the lattice perpendicular to the $[LiAl_2(OH)_6]^+$ layers. $[LiAl_2(OH)_6]Br$ is isostructural with $[LiAl_2(OH)_6]Cl$, while $[LiAl_2(OH)_6]NO_3$ differs only in that two crystallographically distinct O atom positions were identified around the central N atom. This leads to the generation of two partially occupied overlapping NO_3^- ions related by a 180° rotation in the *ab* plane. In the hydrated intercalate, there is significant disorder between the Cl^- anions and the cointercalated water molecules. These intercalation compounds represent rare examples of layered double hydroxides in which the metal cations are ordered within the hydroxide layers. As the structures of these intercalates are not generally known and are difficult to determine by conventional diffraction techniques, a method of predicting them and thus determining the interactions between the host layers and the intercalated guests would be a tool of considerable interest.

Computational techniques have become a valuable tool in understanding the structures of organic,[9] biological,[10] and polymeric systems.[11] Recent molecular mechanics studies have centered on conformational analysis in systems as diverse as poly(ferrocenylsilanes)[12,13]

[†] University of Oxford.
[‡] Curtin University of Technology.

(1) Beina, M. *CEA-PLS Newsl.* **1992**, *3*, 10.
(2) Kokot, Z. *Pharmazie* **1988**, *43*, 249.
(3) Cavani, F.; Trifiro, E.; Vaccari, A. *Catal. Today* **1991**, *11*, 173.
(4) Zigan, F.; Joswig, W.; Burger, N. *Z. Kristallogr.* **1978**, *148*, 255.
(5) Megaw, H. D. *Z. Kristallogr.* **1934**, *87*, 185.
(6) Bosmans, H. J. *Acta Crystallogr.* **1970**, *B26*, 649.
(7) Saalfeld, H.; Wedde, M. *Z. Kristallogr.* **1974**, *139*, 129.
(8) Besserguenev, A. V.; Fogg, A. M.; Price, S. J.; Francis, R. J.; O'Hare, D.; Isupov, V. P.; Tolochko, B. P. *Chem. Mater.* **1997**, *9*, 241.
(9) Desiraju, G. R. *Crystal Engineering: The Design of Organic Solids*; Elsevier: Amsterdam, 1989.
(10) Li, H.; Poulos, T. L. *Acta Crystallogr.* **1995**, *D51*, 21.
(11) Ferro, D. R.; Ragazzi, M.; Bruckner, S.; Meille, S. V. *Macromol. Symp.* **1995**, *89*, 529.
(12) Barlow, S.; Rohl, A. L.; Shi, S.; Freeman, C. M.; O'Hare, D. *J. Am. Chem. Soc.* **1996**, *118*, 7578.
(13) Barlow, S.; Rohl, A. L.; O'Hare, D. *Chem. Commun.* **1996**, 257.

10.1021/cm990066x CCC: $18.00
Published on Web 04/17/1999

and carbohydrates.[14,15] In inorganic systems, computer modeling has been successfully used to confirm experimental observations on the swelling and diffusion in clay minerals.[16−18] Previous computer simulations of layered double hydroxides have been carried out for inorganic and organic intercalates of the Mg/Al system.[19,20] Successful simulations using the Dreiding force field were able to produce excellent agreement between the experimental and calculated interlayer distances, allowing the orientation of the guests to be determined. However, as the structures of these intercalates had not been fully characterized experimentally, it was not possible to confirm the accuracy of the simulated structure. In this study, we aim to reproduce known structures of layered double hydroxides and then go on to use the same set of potentials to predict structures which have not been determined previously.

Molecular modeling studies have also been carried out on gibbsite. In one such study, the structure of gibbsite was adequately reproduced using the cff91 force field, though a significant shift in the layer positions away from the experimental positions was observed.[21] A second study looked at the effect of the inclusion of alkali metal ions on the morphology of gibbsite.[22] The force field used was based on the Born ionic model of solids incorporating the polarization of oxygen atoms and was able to reproduce the known crystal structures of gibbsite and bayerite. It was also shown that sodium, potassium and cesium cations can replace one of the six crystallographically different protons in the structure upon incorporation into the lattice. These calculations also indicated that the inclusion of lithium cations into gibbsite is thermodynamically favorable, as has been confirmed by the facile intercalation of lithium salts into the lattice.

Calculation Section

The structures and energies of the intercalation compounds considered in this work were calculated using molecular mechanics. This method requires the availability of interatomic potentials for all interactions within the lattices.

Potentials. The potentials used in the simulation of the layers are those derived for gibbsite[22] augmented with an additional Li−O potential.[23] The long-range Coulombic interactions, due to the fixed charges on the atoms, were evaluated using an Ewald summation.[24] Buckingham potentials, consisting of a repulsive exponential and an attractive dispersion term between pairs of ions, describe the short-range nonbonded interactions. The Dick−Overhauser shell model was used to model the polarization of the oxygen atoms in the lattice.[25] The potentials used are listed in Table 1, since the gibbsite potentials are not given in ref 22.

Table 1. Potential Parameters Used for the Long Range Interactions in the Layers of $[LiAl_2(OH)_6]X$ (X = Cl, Br, NO_3)

(a) Buckingham: $V(r) = A \exp(-r/\rho) - Cr^{-6}$

interaction	A (eV)	ρ (Å)	C (eVÅ^6)
Al−O	1360.00	0.29912	
Li−O	497.1661	0.29630	
H−O	262.276494	0.268459	
O−O	22764.30	0.14900	27.88

(b) Morse: $V = D_e(\{1 - \exp[-\beta(r - r_0)]\}^2 - 1)$

interaction	D_e (eV)	β (Å)$^{-1}$	r_0 (Å)
H−O	5.539	3.110064	0.97979

(c) Spring (core-shell): $^1/_2k_2r^2$

atom	k_2 (eV Å^{-2})
O	74.92

(d) Coulombic Charges

Al	+3	O (core)	+1.3741
Li	+1	O (shell)	−2.8690
		H	+0.4949

The intramolecular potentials for the guest anions were taken from previous simulations involving NO_3^-,[23] SO_4^{2-},[26] CO_3^{2-},[27] and $C_2O_4^{2-}$.[28] Those that are not listed in the literature are summarized in Table 2.

The interatomic interactions between the guest anions and the hydroxide groups of the layers and the guests themselves are described by Lennard−Jones potentials of the form $Ar^{-9} - Br^{-6}$. These potentials were derived using the extensible systematic force field (ESFF)[12] in the InsightII software package.[29] This force field uses a rule-based algorithm to determine a potential parameter set for a given system with the resulting parameters used to generate the potentials which are detailed in Table 3.

Calculations. The general utility lattice program (GULP) uses symmetry-adapted algorithms in the simulation of three-dimensional inorganic and organic systems with fully flexible molecules.[30] This use of symmetry accelerates the energy and derivative calculations leading to increased computational efficiency relative to standard algorithms. All the lattice optimizations discussed in this paper were carried out using GULP. It should be noted that the GULP lattice energies reported here are in fact the calculated potential energy of the unit cells.

Experimental Details

Synthesis. $[LiAl_2(OH)_6]X.nH_2O$ (X = Cl^-, Br^-, NO_3^-) was prepared by stirring a suspension of gibbsite in an aqueous

(14) Martín-Pastor, M.; Espinosa, J. F.; Asensio, J. L.; Jiménez-Barbero, J. *Carbohydr. Res.* **1997**, *298*, 15.
(15) Asensio, J. L.; Martín-Pastor, M.; Jiménez-Barbero, J. *Theochem.− J. Mol. Struct.* **1997**, *395−496*, 245.
(16) Boek, E. S.; Coveney, P. V.; Skipper, N. T. *J. Am. Chem. Soc.* **1995**, *117*, 12608.
(17) Boek, E. S.; Coveney, P. V.; Skipper, N. T. *Langmuir* **1995**, *11*, 4629.
(18) Yi, X.; Shing, K. S.; Sahimi, M. *AIChE J.* **1995**, *41*, 456.
(19) King, J.; Jones, W. *Mol. Cryst. Liq. Cryst.* **1992**, *211*, 257.
(20) Aicken, A. M.; Bell, I. S.; Coveney, P. V.; Jones, W. *Adv. Mater.* **1997**, *9*, 496.
(21) Teppen, B. J.; Rasmussen, K.; Bertsch, P. M.; Miller, D. M.; Schäfer, L. *J. Phys. Chem.* **1997**, *101*, 1597.
(22) Lee, M.; Rohl, A. L.; Gale, J. D.; Parkinson, G. M.; Lincoln, F. J. *Chem. Eng. Res. Des.* **1996**, *74A*, 739.
(23) Gale, J. D. Personal communication, 1997.
(24) Dick, B. G.; Overhauser, A. W. *Phys. Rev.* **1958**, *112*, 90−103.
(25) Ewald, P. P. *Ann. Phys.* **1921**, *64*, 253.
(26) Allen, N. L.; Rohl, A. L.; Gay, D. H.; Catlow, C. R. A.; Davey, R. J.; Mackrodt, W. C. *Faraday Discuss.* **1993**, *95*, 273.
(27) Pavese, A.; Catti, M.; Parker, S. C.; Wall, A. *Phys. Chem. Miner.* **1996**, *23*, 89.
(28) *Consistent Valence Force field, InsightII Molecular Modelling System*; MSI: San Diego, 1994.
(29) *InsightII Software Package*; MSI Simulations Inc.: San Diego, 1994.
(30) Gale, J. D. *J. Chem. Soc., Faraday Trans.* **1997**, *93*, 629.

Table 2. Intramolecular Potentials Used To Describe the Nitrate and Oxalate Guest Anions

(a) NO_3^-

(i) Harmonic: $^1/_2k_2(r - r_0)^2 + {}^1/_2k_3(r - r_0)^3 + {}^1/_2k_4(r - r_0)^4$

interaction	k_2 (eV Å^{-2})	k_3 (eV Å^{-3})	k_4 (eV Å^{-4})	r_0 (Å)
N−O	50.6370	−408.2327	2779.8844	1.2645

(ii) Three-Body Harmonic: $^1/_2k_2(\theta - \theta_0)^2 + {}^1/_6k_3(\theta - \theta_0)^3 + {}^1/_{12}k_4(\theta - \theta_0)^4$

interaction	k_2 (eV rad^{-2})	k_3 (eV rad^{-3})	k_4 (eV rad^{-4})	θ_0
O−N−O	10.2547	23.9655	74.9604	120

(iii) Torsion: $k(1 + \cos(\text{nphase}(\phi - \phi_0)))$

interaction	k (eV)	nphase	ϕ_0
O−N−O−O	0.623163	+1	0

(iv) Coulombic Charges

N	+0.8774	O	−0.6256

(b) $C_2O_4^{2-}$

(i) Harmonic: $^1/_2k_2(r - r_0)^2$

interaction	k_2 (eV Å^{-2})	interaction	k_2 (eV Å^{-2})
C−O	46.8331	C−C	23.12

(ii) Three-Body Harmonic: $V = {}^1/_2k_2(\theta - \theta_0)^2$

interaction	k_2 (eV rad^{-2})	θ_0
O−C−O	12.5756	123
O−C−C	136.0	120

(iii) Torsion: $k(1 + \cos(\text{nphase}(\phi - \phi_0)))$

interaction	k (eV)	nphase	ϕ_0
C−C−O−O	5	+2	180

(iv) Coulombic Charges

C	+0.378	O	−0.689

Table 3. Lennard−Jones Potential Parameters Used To Describe the Interatomic Interactions between the Guest Anions and the Hydroxide Groups in the $[LiAl_2(OH)_6]^+$ Layers

interaction	A (kcal Å^9)	B (kcal Å^6)
	(a) $[LiAl_2(OH)_6]Cl$	
Cl−O	91497	1432
Cl−H	6003	189.5
	(b) $[LiAl_2(OH)_6]Br$	
Br−O	144784	2020.8
Br−H	10457	285.9
	(c) $[LiAl_2(OH)_6]NO_3$	
$H-O_{guest}$	768.4	40.72
H−N	888.1	61.30
$O_{layer}-O_{guest}$	16442	384.8
O_{layer}−N	243936	84.2
	(d) $[LiAl_2(OH)_6]_2SO_4$	
$H-O_{guest}$	716.9	47.11
H−S	51003	757.9
$O_{layer}-O_{guest}$	26954	494.7
O_{layer}−S	503399	4275.1
	(e) $[LiAl_2(OH)_6]_2CO_3$, $[LiAl_2(OH)_6]_2C_2O_4$	
$H-O_{guest}$	670.8	43.30
H−C	950.9	52.07
$O_{layer}-O_{guest}$	16585	450.5
O_{layer}−C	20834	499.8

solution containing a 4-fold molar excess of the required lithium salt at 90 °C overnight. The first stage ion exchange intercalates were synthesized by the reaction of $[LiAl_2(OH)_6]$-$Cl\cdot H_2O$ with a 3-fold molar excess of either Na_2CO_3, Na_2SO_4, or $Na_2C_2O_4$ in aqueous solution at room temperature for 1 h. The dehydrated analogues of all the intercalates were prepared by heating the initial intercalate under vacuum at 100 °C for 6 h.

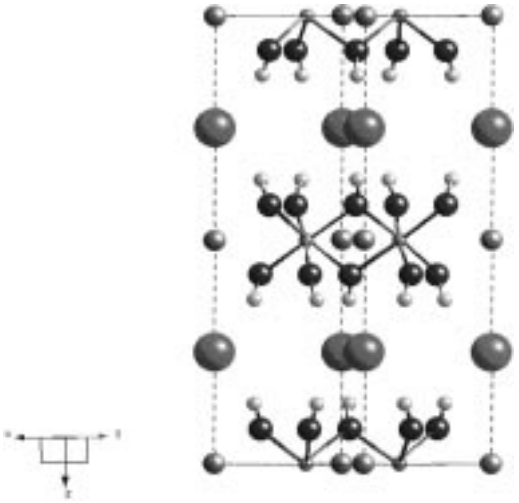

Figure 1. The calculated structure of $[LiAl_2(OH)_6]Cl$.

Table 4. Comparison of the Observed and Calculated Parameters for the Optimization of $[LiAl_2(OH)_6]Cl$

parameter	observed	calculated	difference
a (Å)	5.10005(8)	5.0639	0.03615
c (Å)	14.2994(3)	14.7364	−0.4370
volume (Å^3)	322.10(9)	327.25	−29.9
$O_{x,y}$	0.6350(2)	0.6358	−0.0008
$O_{z,y}$	0.5672(7)	0.5781	−0.0109
H_x	0.6879(5)	0.6851	0.0028
H_z	0.6335(1)	0.6338	−0.0003

Measurements. Powder X-ray diffraction patterns were recorded on either a Siemens D5000 or a Philips PW 1729 diffractometer using Cu Kα radiation. TGA measurements were performed on a STA-1500, using a heating rate of 5 °C/min between 25 and 400 °C under static air.

Results and Discussion

$[LiAl_2(OH)_6]Cl$. The unit cell of $[LiAl_2(OH)_6]Cl$ was minimized using GULP utilizing both the full hexagonal symmetry (space group $P6_3/mcm$) and the equivalent $P1$ representation. In each case the refined structure was used as the starting model.[8] In both cases, the calculations optimized to the same structure and the calculated lattice parameters were in excellent agreement with those obtained from the structural refinement, with the c parameter showing a 3% increase in the optimized structure. The use of the hexagonal symmetry of the system in the calculations confines all but the hydroxide groups to special positions, though in the relaxed structure the shift in their fractional coordinates is minimal. The calculated structure is shown in Figure 1. The observed and calculated parameters for $[LiAl_2(OH)_6]Cl$ are summarized in Table 4. To determine whether this structure represents the global minimum, further minimizations were carried out using the $P1$ representation of the structure in which the Cl^- ion was systematically moved through the interlayer space at $z = 0.25$ in steps of $0.05a$. The positions of the Cl^- ions were fixed relative to an Al^{3+} ion in each $[LiAl_2(OH)_6]^+$ layer, and the rest of the structure was minimized for each Cl^- ion position. From the resulting energy surface (Figure 2) it can be seen that the minimum energy position corresponds to a Cl^- position of (0, 0, 0.25), as was found in the refined structure, though six secondary

Table 5. Summary of Parameters Obtained on Optimization of the Structures of $[LiAl_2(OH)_6]X$ (X = Br, NO_3)[a]

	experimental		calculated		
compound	*a* (Å)	*c* (Å)	*a* (Å)	*c* (Å)	lattice energy (eV)
$[LiAl_2(OH)_6]Br$	5.0996(1)	14.9461(6)	5.0705	15.4739	−341.9971
$[LiAl_2(OH)_6]NO_3$	5.10917(8)	14.3738(3)	5.0702	14.1540	−341.6226

[a] Esds are in parentheses. In all cases the cells are hexagonal and based on a two-layer model.

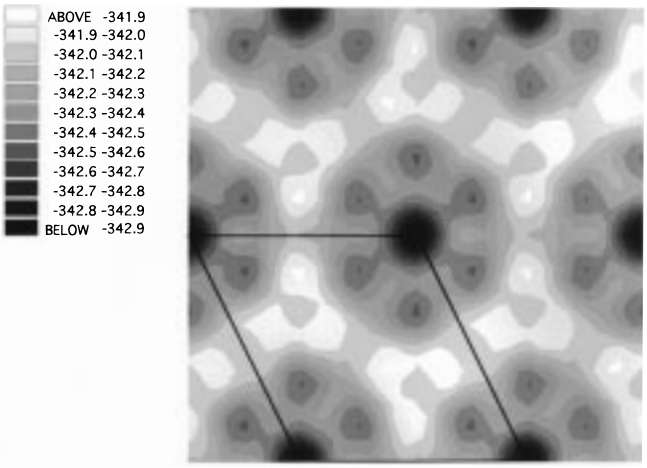

Figure 2. Plot of lattice energy (eV) as the Cl^- anion is moved in the *ab* plane at $z = 0.25$ of $[LiAl_2(OH)_6]Cl$.

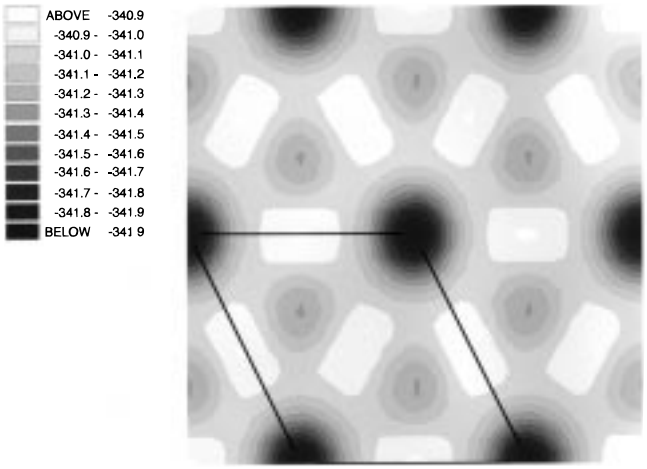

Figure 3. Plot of lattice energy (eV) as the Br^- anion is moved in the *ab* plane at $z = 0.25$ of $[LiAl_2(OH)_6]Br$.

minima around this site are apparent. These correspond to the six sites found for the nitrate O atoms in $[LiAl_2(OH)_6]NO_3$. Further minima are apparent at ($^1/_3$, $^2/_3$, 0.25) and ($^2/_3$, $^1/_3$, 0.25) corresponding to the formation of ···Al···Cl···Al···Cl··· chains analogous to those between the lithium and chloride ions at the global minimum. If the Cl^- ions are displaced from the $z = 0.25$ or $z = 0.75$ planes prior to minimization, they return to these planes on optimization.

$[LiAl_2(OH)_6]Br$. The isostructural intercalate, $[LiAl_2(OH)_6]Br$, was optimized using both the full symmetry and *P*1 representations starting from the refined structure. As for the chloride intercalate, both structural models minimized to the same final lattice energy with the *a* lattice parameter remaining unaltered and the *c* lattice parameter showing a 3.5% increase relative to the experimentally determined structure. The parameters from the minimizations are summarized in Table 5. The energy map corresponding to the movement of the bromide ion between the layers was calculated analogously to that for $[LiAl_2(OH)_6]Cl$ and is shown in Figure 3. It can be seen that the experimentally observed structure with Br at (0, 0, 0.25) is the global minimum, with two secondary minima at ($^1/_3$, $^2/_3$, 0.25) and ($^2/_3$, $^1/_3$, 0.25) corresponding to the bromide ion forming ···Al···Br···Al···Br··· chains through the lattice instead of the ···Li···Br···Li···Br··· chains in the minimum energy structure. The six secondary minima observed around (0, 0, 0.25) observed in the chloride intercalate have disappeared, presumably because of the larger radius of the Br^- anion.

$[LiAl_2(OH)_6]NO_3$. In the refined structure of $[LiAl_2(OH)_6]NO_3$, the N atom was found to occupy the same site as the halide anions, with the two O atom positions around the N atom leading to two nitrate anions related by a 180° rotation in the ab plane existing in a disordered structure. Refinement of the fractional occupancies of the two nitrate orientations using the experimental data indicated that one orientation dominated with 85% occupancy.[8] This disorder reduces the symmetry of the structure to $P6_3/m$. Optimization of the refined structure using this symmetry and the analogous *P*1 representations yielded the same final lattice energies and lattice parameters. The *a* lattice parameter was reduced by less than 1% relative to the refined structure and the *c* lattice parameter by 1.5%. The results from the calculations are summarized in Table 5. A further series of calculations were performed on a structure containing one nitrate ion in the $P6_3/m$ representation in which the anion was systematically rotated in 5° steps through 120° starting from the least occupied orientation in the refined structure. In these calculations, the positions of the N and O atoms of the guest were fixed relative to the aluminum cations in the layers, and the hydroxides were allowed to relax. A comparison of the initial and minimized lattice energies for each step of the rotation is shown in Figure 4. It can be seen that while the initial lattice energies vary smoothly as the nitrate anion is rotated, the relaxed structures show only two different lattice energies. On minimization, the hydroxide layers relax, leading to the adoption of one of the two experimentally observed structures. The lower energy orientation corresponds to the one with the highest fractional occupancy in the experimentally determined structure. From the difference in energy between these two orientations, the barrier to rotation of the nitrate anion in $[LiAl_2(OH)_6]NO_3$ can be determined to be 0.068 eV (6.55 kJ mol^{-1}). This is significantly above kT for room temperature, indicating that the NO_3^- anion is not rotating, so the two different orientations of the ion will be frozen out in the intercalate. Assuming a Boltzmann two-level energy with a energy gap of 0.068 eV, we estimate the ratio of nitrate orientations to be 89:11. This is in remarkably good agreement with the 85:15 ratio obtained experimentally from the powder X-ray data.

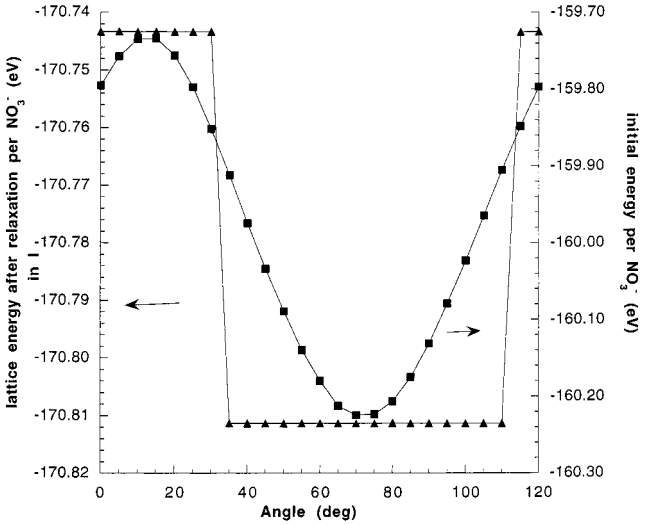

Figure 4. Variation of the lattice energy per nitrate anion for $[LiAl_2(OH)_6]NO_3$ as a function of the orientation of the NO_3^- ion before (■) and after optimization (▲) of the unit cell. The total lattice energy is twice the plotted energy since there are two nitrate ions per unit cell.

We have shown that molecular mechanics can satisfactorily reproduce the experimentally determined structures of the layered double hydroxides $[LiAl_2(OH)_6]X$ (X = Cl^-, Br^-, NO_3^-). Both the structures and the energetics of these compounds were reproduced with a high degree of accuracy. Following the success of this study, we applied the same principles to the related dianionic intercalates $[LiAl_2(OH)_6]_2A$ (A = CO_3^{2-}, SO_4^{2-}, $C_2O_4^{2-}$), whose structures have not been determined previously.

$[LiAl_2(OH)_6]_2A$. Ion exchange reactions of $[LiAl_2(OH)_6]Cl\cdot H_2O$ with salts of dianions such as CO_3^{2-}, SO_4^{2-} and $C_2O_4^{2-}$ occur very readily at room temperature, leading to intercalates of the general formula $[LiAl_2(OH)_6]_2A\cdot nH_2O$. As for the intercalates with monoanions, the cointercalated water molecules can be readily removed under vacuum at 80 °C, leaving $[LiAl_2(OH)_6]_2A$. However, these compounds are not as crystalline as their monoanionic counterparts, so their structures have not been solved using conventional techniques and it is only possible to extract interlayer separations from the diffraction patterns for comparison with the calculated structures. These intercalates contain half the number of guest anions, so in the trial structures, the dianions can be disordered with half-occupancy on each Cl site, leaving the *a* lattice parameter unaltered. Structural optimizations were carried out as before using *P*1 representations of the model structure for $[LiAl_2(OH)_6]_2CO_3$, $[LiAl_2(OH)_6]_2SO_4$, and $[LiAl_2(OH)_6]_2C_2O_4$ in which the anions are disordered over each chloride site with half-occupancy.

Partial occupancies are incorporated within GULP by use of a mean field model. In this approach, the interaction between any two species simply becomes scaled by the product of their site occupancies. Similarly for a three-body interaction, the product of all three site occupancies is used to scale the interaction energy. Where two atoms share the same crystallographic site, these are then automatically constrained to move together and thus behave as a pseudoatom with the averaged properties of the two or more component species.

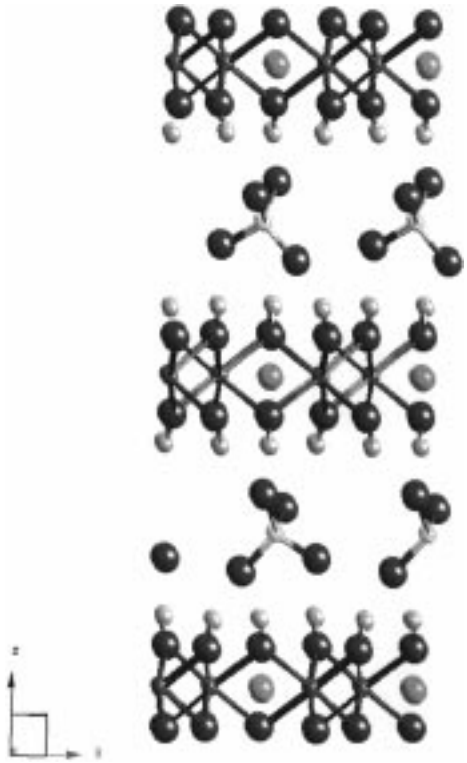

Figure 5. Minimized structure of $[LiAl_2(OH)_6]_2SO_4$.

The mean field model provides a reasonable representation of systems where the distribution of ions is highly disordered. It will clearly not reproduce local distortions in the environment about individual ions but will yield an averaged environment in a similar way to a diffraction study. Macroscopic properties, such as elastic constants and thermal expansion, will be better reproduced than the local geometry in this type of approach. However, excess quantities may be overestimated as local distortions can work cooperatively to achieve this.

$[LiAl_2(OH)_6]_2SO_4$. Optimization of the disordered structure of $[LiAl_2(OH)_6]_2SO_4$ gave an interlayer separation of 9.0 Å, which compares very favorably to the experimental value of 8.8 Å. The hexagonal nature of the cell was retained on relaxation, despite the *P*1 symmetry used in the calculations, though the SO_4^{2-} anions were displaced fractionally from the chloride site. The sulfate anions are oriented such that two of the O atoms occupy positions which are analogous to two of the six O atom positions in $[LiAl_2(OH)_6]NO_3$ in their location with respect to the hydroxide groups of the layer. The tetrahedral geometry of the SO_4^{2-} anions means that the two O atoms which interact with the second layer occupy positions midway between those found in $[LiAl_2(OH)_6]NO_3$. This orientation is one of two which have previously been proposed for sulfate anions in layered double hydroxides.[31,32] In the other possibility, three oxygen atoms are directed toward one layer, giving a trigonal pyramidal orientation. The former case requires a smaller interlayer separation, so it would seem reasonable that this would be adopted in the minimum energy structure. The minimized structure is shown in Figure 5. The results from the calculations

(31) Brindley, G. W.; Kikkawa, S. *Clays Clay Miner.* **1980**, *28*, 87.
(32) Bish, D. L. *Bull. Miner.* **1980**, *103*, 170.

Table 6. Summary of Parameters Obtained on Optimization of the Structures of $[LiAl_2(OH)_6]_2A$ ($A = CO_3^{2-}, SO_4^{2-}$)[a]

		calculated		
compound	expl *c* (Å)	*a* (Å)	*c* (Å)	lattice energy (eV)
$[LiAl_2(OH)_6]_2SO_4$	17.6	5.10	17.97	−349.8993
$[LiAl_2(OH)_6]_2CO_3$	12.8	5.10	13.08	−624.6217

[a] All cells are based on a two-layer model.

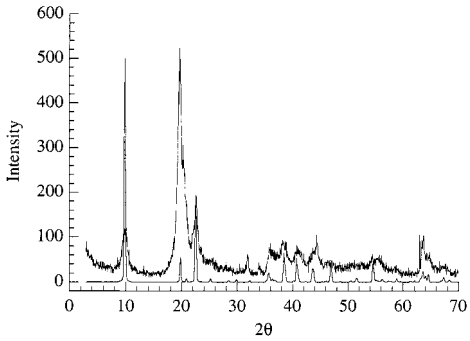

Figure 6. Comparison of the observed and calculated diffraction patterns for $[LiAl_2(OH)_6]_2SO_4$.

are summarized in Table 6. From the optimized structure an X-ray diffraction pattern was calculated using the InsightII software package and is shown with the experimental pattern in Figure 6 for comparison. It can be seen that while there is qualitative agreement between the two diffraction patterns, the experimental data is of too poor quality for any structure determination to be undertaken. Despite this, it is likely that the unit cell is correct and the model predicted in the calculation is a reasonable representation of the local structure.

$[LiAl_2(OH)_6]_2CO_3$. The disordered structural representation of $[LiAl_2(OH)_6]_2CO_3$ with the carbonate ions oriented with their molecular plane parallel to the layers was minimized, giving a cell in which the interlayer separation was 6.6 Å. This can be compared with the experimentally observed value of 6.4 Å. The hexagonal nature of the cell was retained despite *P*1 symmetry being used in the calculation. The orientation of the CO_3^{2-} anion in the optimized structure is the same as that adopted by NO_3^- in the lowest energy orientation in $[LiAl_2(OH)_6]NO_3$. The lattice energy and cell parameters from the calculations are given in Table 6.

$[LiAl_2(OH)_6]_2C_2O_4$. The structure of $[LiAl_2(OH)_6]_2C_2O_4$ was optimized starting from three different orientations of the $C_2O_4^{2-}$ guest within the host lattice: the principal axis perpendicular to the layers or the axis parallel to them with the molecular plane either parallel or perpendicular to the layers. These orientations are shown schematically in Figure 7. For the disordered structure, it was found that if the principal axis of the oxalate anion was parallel to the layers, the optimized structure contained anions with their molecular planes essentially perpendicular to the layers regardless of the initial orientation. This gave a calculated layer separation of 8.6 Å, and there is significant distortion of the cell from the hexagonal lattice on minimization, giving a triclinic cell. If the unit cell is constrained to be hexagonal, the calculated layer separation is reduced to 8.3 Å. When the principal axis was initially perpendicular to the layers, this orientation was maintained in the relaxed structure, giving a phase with an interlayer separation of 9.05 Å with the cell retaining its hexagonal character. This structure was, however, 0.15 eV (14.5 kJ mol^{-1}) higher in energy than for the other orientation. The parameters obtained from the optimizations are summarized in Table 7. The experimental layer separation is 8.65 Å, indicating that the lower energy structure is the one adopted in $[LiAl_2(OH)_6]_2C_2O_4$. This observation is particularly surprising, as it represents an increase in the layer separation from 8.2 Å on removal of the cointercalated water rather than the expected decrease.

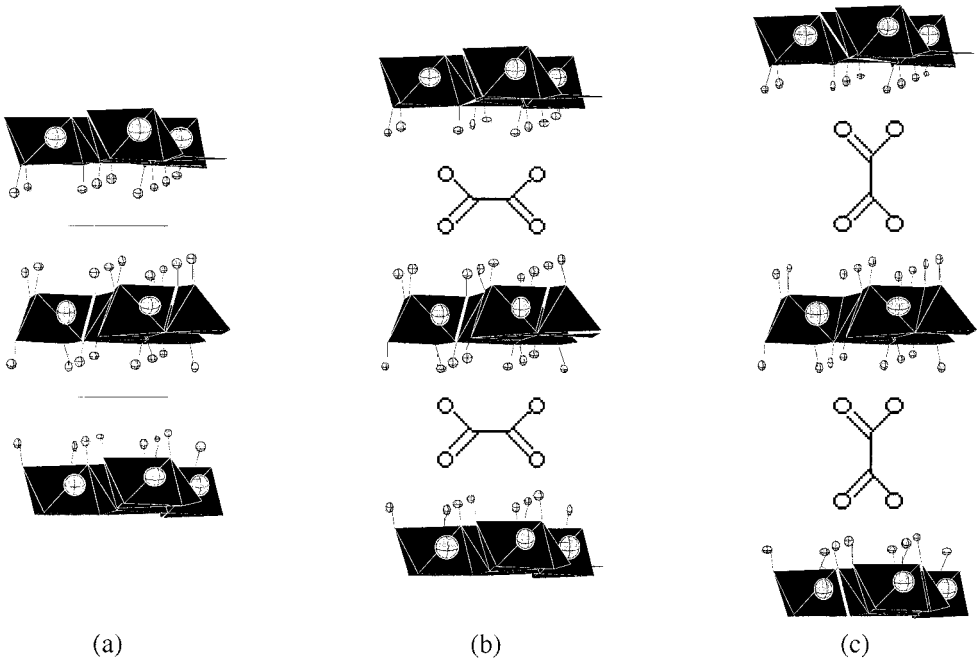

Figure 7. Schematic diagram showing the different orientations of the oxalate anion used as starting points in the structural minimizations of $[LiAl_2(OH)_6]_2C_2O_4$ (a) principal axis and molecular plane parallel to the layers, (b) principal axis parallel and molecular plane perpendicular to the layers, and (c) principal axis and molecular plane perpendicular to the layers.

Table 7. Summary of the Parameters Obtained on Optimization of the Structure of $[LiAl_2(OH)_6]_2C_2O_4$[a]

$[LiAl_2(OH)_6]_2C_2O_4$	*a* (Å)	*b* (Å)	*c* (Å)	α	*β*	*γ*	lattice energy (eV)
from Figure 7a,b[b]	5.07	5.05	17.22	100.0	91.10	120.0	−341.1306
from Figure 7c[c]	5.06	5.07	18.03	88.36	91.18	120.1	−340.9796

[a] All cells are based on a two-layer model. The experimental *c* parameter for $[LiAl_2(OH)_6]_2C_2O_4$ is 16.2 Å. [b] Starting from the orientations shown in Figure 7, parts a and b. [c] Starting from the orientation shown in Figure 7c.

Figure 8. Minimized structure of $[LiAl_2(OH)_6]_2C_2O_4$.

A comparison of the X-ray diffraction patterns calculated from these structures indicates that the triclinic cell is in better agreement with the experimental data, though due to the low crystallinity of the sample it is not possible to draw any firm conclusions from this analysis.

This leads us to believe that while we cannot solve the structure of $[LiAl_2(OH)_6]_2C_2O_4$, it is likely that it is significantly distorted from the hexagonal cell found for $[LiAl_2(OH)_6]Cl$ and has significant disorder of the guest anions over each Cl site each oriented with the principal axis parallel and the molecular plane perpendicular to the $[LiAl_2(OH)_6]^+$ layers.

The orientation of oxalate anions within hydrated LDHs appears to vary depending on the layer charge and amount of cointercalated water. For example, the interlayer separation for the oxalate intercalate of a Zn/Al LDH, $[Zn_3Al(OH)_8]_2C_2O_4 \cdot nH_2O$ ($c = 7.8$ Å), indicates that the anions are oriented with their molecular planes parallel to the layers, in contrast to that observed for $[LiAl_2(OH)_6]_2C_2O_4 \cdot nH_2O$.

Conclusions

We have demonstrated that computer simulations of layered double hydroxides can be used to rationalize known structures and provide useful structural information on structures that have not been determined experimentally. The calculated structures are in excellent agreement with those solved by conventional diffraction techniques and can be used to predict guest orientations in other layered double hydroxide intercalates. Work on the simulation of the hydrated structures is underway and will be published at a later date.

Acknowledgment. A.M.F. would like to thank EPSRC for a studentship. This work has been supported under the Australian Government's Cooperative Research Centres Program, and this support is gratefully acknowledged. We would also like to thank Dr. Julian Gale for useful discussions during the course of this work.

CM990066X